Environ. Sci. Technol. **2007**, *41*, 7675−7682

Factors Influencing Mobile Source Particulate Matter Emissions-to-Exposure Relationships in the Boston Urban Area

SUSAN L. GRECO,*,†
ANDREW M. WILSON,‡
STEVEN R. HANNA,† AND
JONATHAN I. LEVY†,‡

Department of Environmental Health, Harvard School of Public Health, and Harvard Center for Risk Analysis, Boston, Massachusetts

Benefit−cost and regulatory impact analyses often use atmospheric dispersion models with coarse resolution to estimate the benefits of proposed mobile source emission control regulations. This approach may bias health estimates or miss important intra-urban variability for primary air pollutants. In this study, we estimate primary fine particulate matter ($PM_{2.5}$) intake fractions (iF; the fraction of a pollutant emitted from a source that is inhaled by the population) for each of 23 398 road segments in the Boston Metro Core area to evaluate the potential for intra-urban variability in the emissions-to-exposure relationship. We estimate iFs using the CAL3QHCR line source model combined with residential populations within 5000 m of each road segment. The annual average values for the road segments range from 0.8 to 53 per million, with a mean of 12 per million. On average, 46% of the total exposure is realized within 200 m of the road segment, though this varies from 0 to 93% largely due to variable population patterns. Our findings indicate the likelihood of substantial intra-urban variability in mobile source primary $PM_{2.5}$ iF that accounting for population movement with time, localized meteorological conditions, and street-canyon configurations would likely increase.

1. Introduction

When evaluating the health effects of motor vehicle emissions in the context of benefit−cost analysis, atmospheric dispersion models are conventionally applied to link emissions with population exposures (*1*). In applying such models, decisions must be made regarding the geographic scope and resolution that would provide accurate and unbiased estimates of exposure, especially in and around urban areas. At present, there is a substantial disconnect in the literature which is difficult to resolve. On the one hand, multiple studies have shown that concentrations of primary pollutants emitted from motor vehicles tend to drop off rapidly with distance from the road (*2*−*4*), with most of the impact observed within hundreds of meters. On the other hand, models conventionally used to examine the impact of mobile source generated fine particulate matter ($PM_{2.5}$) emissions on populations across the United States use coarse geographic resolution (i.e., 36 km × 36 km) (*1*, *5*). These lines of evidence may be consistent (i.e., if small concentration increments influenced large long-range populations), but could also indicate that the approach conventionally used for benefit−cost analysis significantly misstates population exposures. Moreover, even if coarse resolution models yielded reasonable mean estimates, they may miss important local-scale heterogeneity.

The intake fraction (iF) is a useful tool for summarizing the extent to which emissions might impact populations, and can allow us to make the comparisons necessary to address the above questions. The iF is defined as the fraction of a pollutant emitted from a source that is inhaled by a defined population (*6*). Previous studies have provided estimates for mobile source iF in urban areas, but have not examined intra-urban variability that may be related to concentration gradients and highly variable populations around roadways. For example, Greco et al. used a source−receptor matrix that covered the contiguous United States at county-level resolution, demonstrating significant between-county differences in primary $PM_{2.5}$ iF (range across 3080 counties: 0.12−25 per million) but not addressing within-county variations (*7*). Other iF studies had similar (*8*) or even less geographic resolution, relying on the spatial density of the ambient monitoring network (*9*) or using 100 × 100 km grid cells (*10*). One study used a nested grid to combine a Gaussian plume model to estimate short-range (within 100 km of the source) iFs and a wind trajectory model to estimate long-range iFs for diesel PM (*11*), but did not explicitly examine how the iF might vary within an urban area or at small spatial scales.

The goal of this study is to determine whether significant heterogeneity in mobile source primary $PM_{2.5}$ iFs might exist within an urban area and if so, which factors explain this heterogeneity. An obvious limitation in addressing intra-urban variability in mobile source iFs is the fact that there are numerous road segments and configurations, and varying population patterns, making it implausible to apply computational fluid dynamic or artificial neural network models to all situations. Instead, we apply an EPA-recommended line-source model and determine which meteorological and population parameters influence the iF (and over what distance), providing guidance to future, more-refined modeling efforts. To evaluate influential parameters, we first consider the influence of meteorology holding population fixed, then the influence of population patterns holding meteorology spatially constant, and finally consider qualitatively the interactions between spatial patterns of meteorology and population within an urban core.

2. Methods

In order to investigate the potential for intra-urban variability in mobile source iFs, we consider all road segments within an area defined as the Boston Metro Core (Supporting Information Figure S-1). We estimate intake fraction, iF_{jk}, for each of the j = 1:23 398 road segments in the Boston Metro Core area for each of k = 1:8715 h in 1 year according to eq 1.

$$iF_{jk} = \Sigma_i(P_{ij}\,\Delta C_{ik}) \times BR/Q \qquad (1)$$

P_{ij} refers to the population contained within region i around the road segment j. While this term could theoretically

* Corresponding author current address: Abt Associates Inc., Environment & Resources Division, 4800 Montgomery Lane, Suite 600, Bethesda, MD 20814; phone: 301.347.5127; fax: 301.828.9737; e-mail: greco.sue@gmail.com.
† Department of Environmental Health, Harvard School of Public Health.
‡ Harvard Center for Risk Analysis.

10.1021/es062213f CCC: $37.00 © 2007 American Chemical Society
Published on Web 11/13/2007

be indexed by k as well, population time−activity patterns are not available at fine temporal and spatial resolution. ΔC_{ik} (in μg m^{-3}) refers to the change in ambient $PM_{2.5}$ concentration attributable to the mobile source emissions from the road segment averaged over the region i for the hour k. Undoubtedly this term would vary by j based on road and building configurations, but within this study we presume similar roadway characteristics for each road segment, as more refined road-specific modeling was implausible in this context. In all instances, a nominal breathing rate, BR, of 20 m^3 d^{-1} and fixed mobile source emissions, Q, are employed. Thus, the only terms that change in the iF_{jk} calculation are P_{ij} and ΔC_{ik}, described below under Population Estimates and Line-Source Model, respectively.

The iF in eq 1 represents the total iF. Alternatively stated, it is the iF that occurs within 5000 m, the spatial extent of the model domain. While some exposure could occur beyond 5000 m, this was beyond the range of the selected line-source model. To determine distances where a given proportion of the iF is met, we define another term. The fraction of total exposure, fTE(r), refers to the percent of the total iF that is met within a specified radius of the road segment. For example, fTE(200 m) is calculated by dividing the iF that occurs in 200 m (calculated from eq 1 by restricting the domain to 200 m) by the total iF. In this study, the fTE(5000 m) is 100%.

2.1. Population Estimates. The Boston Metro Core area held 824 440 residents (based on 2000 U.S. Census data) in an area of 165.9 km^2. We used the ESRI ArcGIS (version 9.1) program with an areal interpolation extension developed by the Long Island Breast Cancer Study Project (National Cancer Institute, http://www.healthgis-li.com/researchers/stat_tools.jsp) to obtain residential populations around the road segments. Using the Massachusetts state plane projection, buffers were created around the midpoints of the 23 398 road segments, allowing for the calculation of residential populations within 50, 100, 200, 500, 1000, and 5000 m of each road segment. These regions were chosen to capture significant gradients in concentration at distances from the roadway within 500 m as well as small impacts at larger distances. Populations outside of the Boston Metro Core were included in these calculations. Population data were available at the census block level (the finest resolution data within the U.S. Census), with the assumption of uniform population density within blocks. For the Boston Metro Core, there are 7564 census blocks, ranging in size from 0.000129 to 5.2 km^2. Where the buffers intersected the blocks, the areal interpolation extension multiplied the fraction of the block within each buffer by the total population of the block and summed the result for each buffer.

2.2. Line-Source Model. Due to its past use and validation, ease of implementation, and suitability to investigate the influence of meteorological parameters, we used the CAL3QHCR line-source model to estimate attributable concentrations in eq 1. CAL3QHCR allows for annual hourly meteorological data and is based largely on the CALINE3 model (*12*).

CALINE3 uses a crosswind Gaussian formulation for a line source of finite length to compute the concentration of inert pollutants near highways (*13*). The model has been evaluated against monitored data and other models and found to compare favorably to both (*13*−*15*). CALINE defines the "mixing zone" (zone of uniform emissions and turbulence) as the region over the roadway plus 3 m on each side to account for the plume generated by the wake of moving vehicles (*16*). The Gaussian formulation assumes horizontally homogeneous winds and steady-state meteorological conditions over the model domain. As a result, the model does not perform well during low wind speed conditions when meandering often occurs or during parallel-to-the-road wind conditions (*13*). In this study, no model output was available for wind speeds less than 1 m s^{-1}.

Hourly surface meteorological data for 1994 from Logan Airport (located within the study area in Boston) and upper air data from Chatham, Massachusetts (located approximately 80 km away) were used. This year was based on data availability, though the influence of the meteorological parameters is more important in this context than their actual values. Inputs into CAL3QHCR consisted of hourly resolved wind speed and direction, temperature, Pasquill−Gifford stability class, and urban and rural mixing heights.

The model was run in the urban mode, signifying that just the urban mixing height data were employed. The model is insensitive to mixing heights except for very low values, below 100 m (*12*). Furthermore, in the urban mode, stable stability conditions E and F are not permitted to exist close to the ground. Instead, they are replaced by neutral (D) stability class (*17*). A roughness length of 500 cm corresponding to a central business district area (*18*) and a settling velocity corresponding to a particle size of 2.5 μm were employed. Fixed emissions consisting of a free-flow link with 3600 vehicles/hour and an emission factor of 1 g/vehicle mile traveled (VMT) were used to generate concentrations, with the emission rate then divided back out of the iF_{jk} according to eq 1. A relatively high emission factor was used to provide better model resolution, given linearity of the outputs with respect to emission rate and the fact that iF is estimated per unit emissions.

Road segments (source links) and receptors (population centroids) had to be specified in the CAL3QHCR model. A uniform roadway configuration of 100 m long and 6 m wide, adding the recommended 3 m buffer on each side, was used. This was comparable to the average road length of the 23 398 road segments, which was 94 m. The population was centered on eight radially spaced receptors inside each of the six regions around the midpoints of the road segments described above. The attributable concentration in each region was determined by averaging the model output across these receptors.

2.3. Analysis. To determine which factors might impact the iF, we investigated the model output in two steps. First, to determine the impact of meteorological variables, we held population constant, applying the average uniform population density to the receptor area and running the line-source model for one year to determine the hourly iF. We considered the effect of hourly wind speed, stability class, urban mixing height, and temperature on hourly iF. For continuous independent variables, univariate regression models were constructed, using transformations based on the functional form of the Gaussian plume model. Since stability class is a categorical value, ANOVA was used to determine the relationship between hourly iF and the classes, collapsing stability classes D, E, and F together to be consistent with CAL3QHCR. In addition to total iF, the impact of meteorology was also examined on the partial iFs occurring within 50, 100, 200, 500, and 1000 m. The impact of particle size and roughness length input parameters was examined in a sensitivity analysis.

Second, we used actual populations between 0 and 50 m, 50 and 100 m, 100 and 200 m, 200 and 500 m, 500 and 1000 m, and 1000 and 5000 m of the roadway for road segments and investigated the impact of population density on the annual average iF (presuming that the same meteorology applies to all road segments). To determine which of the 6 population regions around the roads best explained the linear relationship between population and iF, we constructed univariate regression models with iF as a function of each of the population predictors.

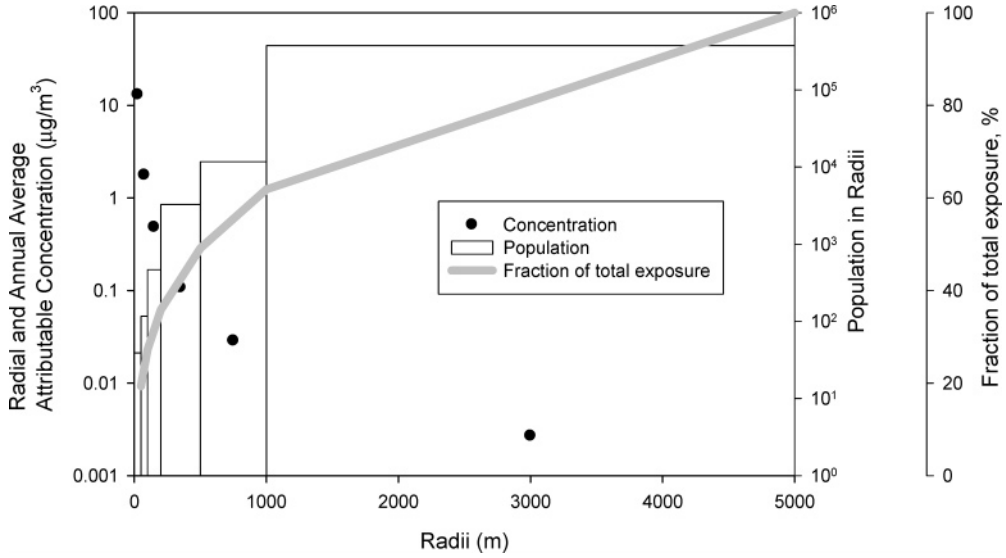

FIGURE 1. Attributable concentration, population, and fraction of total exposure with radial distance from the road. For the uniform population density scheme, the concentration at each of eight receptors around each of the six regions (0−50 m, 50−100 m, 100−200 m, 200−500 m, 500−1000 m, and 1000−5000 m) is averaged over the year. (Note that these concentrations should not be interpreted directly since they result from unit emission inputs to the CAL3QHCR model.) The fraction of total exposure is the normalized cumulative sum product of concentration and population.

TABLE 1. Influence of Wind Speed and Mixing Height on Hourly Intake Fraction[a]

dependent variable	R^2	independent variables	estimate	SE	*p*-value
hourly iF in 100 m	0.92	β_0 (intercept)	1.71×10^{-07}	9.15×10^{-09}	< 0.0001
		β_1 inverse wind speed	1.13×10^{-05}	3.60×10^{-08}	< 0.0001
hourly iF in 200 m	0.92	β_0 (intercept)	2.51×10^{-07}	1.14×10^{-08}	< 0.0001
		β_1 inverse wind speed	1.47×10^{-05}	4.48×10^{-08}	< 0.0001
hourly iF in 500 m	0.88	β_0 (intercept)	3.44×10^{-07}	2.00×10^{-08}	< 0.0001
		β_1 inverse wind speed	2.02×10^{-05}	7.85×10^{-08}	< 0.0001
hourly iF in 1000 m	0.79	β_0 (intercept)	3.74×10^{-07}	3.63×10^{-08}	< 0.0001
		β_1 inverse wind speed	2.57×10^{-05}	1.43×10^{-07}	< 0.0001
hourly iF	0.39	β_0 (intercept)	-2.43×10^{-08}	1.51×10^{-07}	0.87
		β_1 inverse wind speed	4.44×10^{-05}	5.94×10^{-07}	< 0.0001
hourly iF	0.20	β_0 (intercept)	9.06×10^{-06}	8.66×10^{-08}	<0.0001
		β_1 inverse mixing height	2.27×10^{-04}	4.92×10^{-06}	<0.0001
hourly iF	0.54	β_0 (intercept)	-2.00×10^{-07}	1.31×10^{-07}	0.12
		β_1 inverse wind speed	4.21×10^{-05}	5.15×10^{-07}	< 0.0001
		β_2 inverse mixing height	2.02×10^{-04}	3.72×10^{-06}	<0.0001

[a] The hourly iF in 100 m covers the domain from 0 to 100 m. Similarly for the hourly iF in 200, 500, and 1000 m. The hourly iF covers the domain from 0 to 5000 m. Each regression included $n = 8715$ h of data.

3. Results

Summaries of the hourly meteorological parameters that were used as inputs into the CAL3QHCR model and the populations in the six regions (around the midpoint of the road segments) used in our dispersion modeling are shown in the Supporting Information (Tables S-1 and S-2). Table S-2 also displays the population values used in the theoretical uniform population scenario, which are generally similar to the mean by road segment.

Although the modeled hourly attributable concentration (averaged over the year) decreases rapidly with distance from the midpoint of the road (Figure 1), as anticipated, the iF metric considers population, rather than individual, exposures. With theoretical uniform population density in each region, the figure demonstrates that large impacted populations combined with low concentrations can still contribute greatly to total population exposure.

3.1. Impact of Meteorology. First describing the range in intake fractions over time with a fixed uniform population, the mean hourly iF was 9.8 per million, with a range of 1.5 to 300 per million across the 8715 h. As indicated in Supporting Information Figure S-2, the fraction of total exposure that occurs within 200 m of the roadway has a mean value of 43% (range 2−77% across all hours). This would indicate that a modeling domain of 200 m around the roadway, on average, captures less than half of the total impacts, but could potentially capture an insignificant amount or up to three-quarters of the impacts depending upon the meteorological conditions.

In univariate regression models of hourly iF versus meteorological parameters, only wind speed, mixing height, and stability class were found to be influential. A simple linear regression model of hourly iF versus the inverse of wind speed explained about 39% of the variability in this relationship (Table 1, Figure S-3). When the spatial domain was restricted to 100, 200, 500, or 1000 m, the R^2 increased. Outliers are related to hours of extremely low urban mixing heights (less than 16 m). For hourly iF and the inverse of urban mixing height, the R^2 was 20% (Table 1, Figure S-4), but this was increased to 42% if the data were restricted to

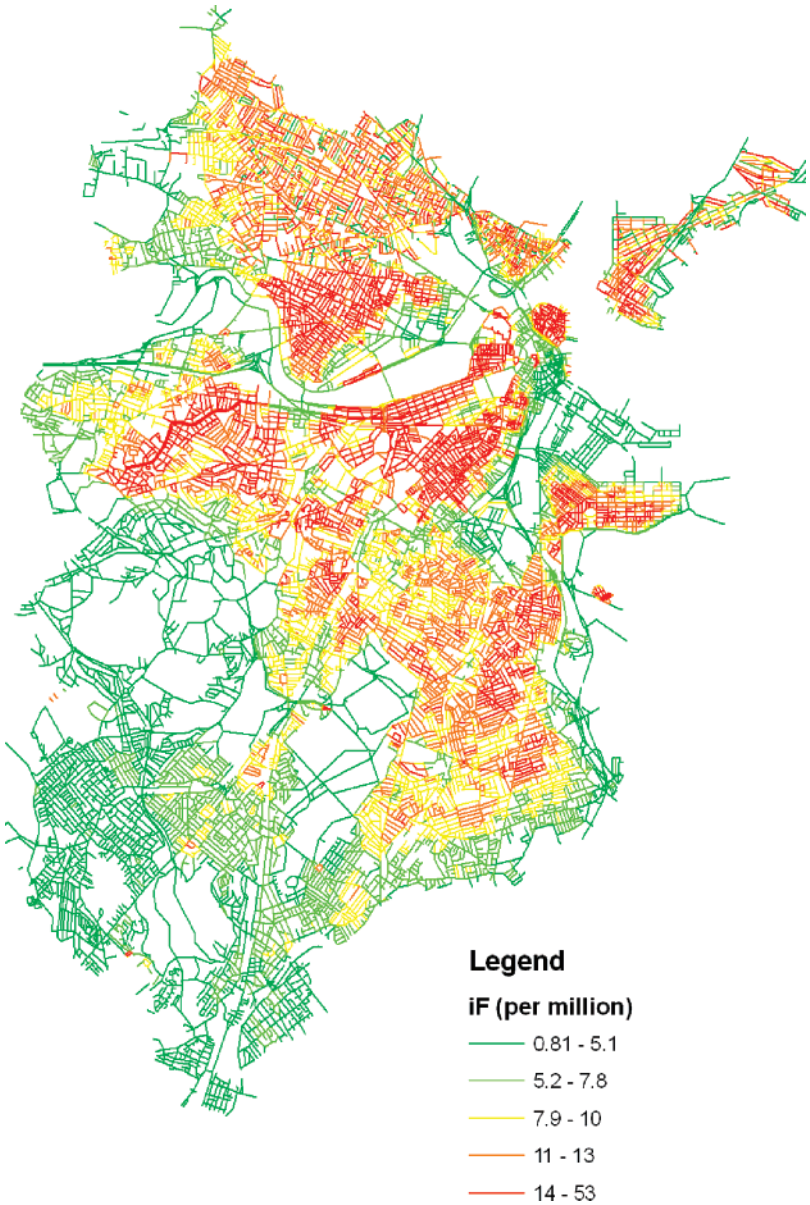

FIGURE 2. Annual average primary $PM_{2.5}$ intake fraction for road segments in the Boston Metro core area.

mixing heights less than 100 m (Table S-3). In a multivariate regression model with inverse wind speed and inverse mixing height across all hours, both predictors are significant and result in an adjusted-R^2 of 54%. The hourly iF varies slightly by stability class category (R^2 < 1%, Figure S-5), with the combined class of D, E, and F having significantly higher hourly iFs than the slightly unstable class C. As a result of diurnal meteorological changes, the iF also varies slightly by hour of day (Figure S-6). Stable stability classes and lower wind speeds tend to occur during the night, resulting in higher iFs at these times.

A sensitivity analysis was conducted for some of the input parameters into the CAL3QHCR model for the uniform population density scheme (Table S-4). In the model, we used an urban roughness length (z_o) for a central business district of 500 cm. Using lower roughness lengths that might be expected in less built-up or rural areas could increase the iF by up to 28% for a z_o of 1 cm. We used a settling velocity corresponding to a particle diameter of 2.5 μm in our model, but tested the sensitivity of the findings. Larger particles (up to 50 μm) decreased the iF by up to 20% because increased settling closer to the roadway did not permit exposures at greater distances from the road, but these particles are not in the respirable fraction of concern, and the model was insensitive to settling velocity for particle diameters smaller than 2.5 μm.

3.2. Impact of Population Distribution. Assuming spatially constant meteorology and using actual population patterns, the mean annual average iF is 12 per million across all road segments (10th and 90th percentiles are 4.9 and 20 per million, respectively, with a range from 0.8 to 53 per million). There are distinct spatial patterns (Figure 2), with high iF areas corresponding to locations of high residential population density within 5000 m around the road segment.

In univariate regression models for iF versus the population in each region (Table 2), populations between 0 and 50, 50 and 100, and 100 and 200 m are all good independent predictors of the annual average iF for each road segment. The predictive power of the regions outside of 200 m decreases significantly, though the regression coefficients remain statistically significant. In addition, while the coefficient for population between 1000 and 5000 m is 3 orders of magnitude below that for populations within 200 m, the population within this annulus is 3 orders of magnitude

TABLE 2. Univariate Regression Models of Annual Average Intake Fraction (Dependent Variable) versus Population in Radial Regions (Actual Population Scheme)[a]

independent variables	R^2	parameter estimate	SE	*p*-value
β_0 (intercept)	0.81	6.29×10^{-06}	2.37×10^{-08}	<0.0001
β_1 population within 50 m		8.77×10^{-08}	2.79×10^{-10}	<0.0001
β_0 (intercept)	0.84	5.27×10^{-06}	2.36×10^{-08}	<0.0001
β_1 population between 50−100 m		3.60×10^{-08}	1.03×10^{-10}	<0.0001
β_0 (intercept)	0.74	4.53×10^{-06}	3.35×10^{-08}	<0.0001
β_1 population between 100−200 m		1.06×10^{-08}	4.10×10^{-11}	<0.0001
β_0 (intercept)	0.60	3.34×10^{-06}	5.09×10^{-08}	<0.0001
β_1 population between 200−500 m		2.00×10^{-09}	1.08×10^{-11}	<0.0001
β_0 (intercept)	0.33	4.69×10^{-06}	7.21×10^{-08}	<0.0001
β_1 population between 500−1000 m		5.34×10^{-10}	4.99×10^{-12}	<0.0001
β_0 (intercept)	0.27	1.50×10^{-06}	1.14×10^{-07}	<0.0001
β_1 population between 1000−5000 m		3.16×10^{-11}	3.39×10^{-13}	<0.0001

[a] For each regression, the number of iF estimates was equal to the number of roads, $n = 23\,398$.

greater (Table S-2), indicating that longer-range domains cannot be excluded.

On average across the hours and road segments, 46% of the total exposure occurs within 200 m of the road segment (10th and 90th percentiles are 28% and 67%, respectively, with a range from 0% to 93%) (Figure 3). Compared to Figure 2, this map shows less distinct patterns. Road segments that are shaded red on both maps correspond to areas that contain large residential populations within the model domain of 5000 m, with a large fraction of the population within 200 m. Road segments that are shaded green on both maps reflect a low population density within 5000 m, but a large fraction of this population outside of 200 m.

4. Discussion

We found that annual average mobile source iFs for $PM_{2.5}$ in the Boston Metro core area varied over 2 orders of magnitude across the road segments when residential populations were considered, and significant variability in daily iF was related to meteorological factors, independent of population.

A critical question is whether the simplifying assumptions within our analysis contributed to significant errors in either the degree of intra-urban variability or the average $PM_{2.5}$ intake fraction for mobile sources in an urban area. We would be particularly concerned about assumptions that overstated variability, since our study seeks to determine if variability is significant enough to be of concern in future analyses. We summarize our major assumptions in Table 3, and briefly describe each below.

In the uniform population density scheme, we found wind speed to be the most important meteorological predictor of hourly intake fractions, though the iF also varied by mixing height, and to a lesser extent, stability class. Since we assumed that the population was uniformly radially distributed in each region, wind direction was rendered insignificant since the attributable concentrations from every wind direction would impact the same population. Accounting for actual population patterns could make wind direction an important meteorological predictor of the intake fraction, although it has been argued previously that upwind and downwind situations, which could increase or decrease the iF, might cancel out for a large number of sources (*11*).

We assumed identical meteorology for each road segment, but in actuality, wind speed in an urban area can vary significantly from one street to another and might differ from the central site monitor. For example, in urban areas, the average of wind speeds close to the ground has been found to be a factor of 3 lower than those measured at airport monitoring stations outside the city (*19*). As it is precisely those road segments with high population density that would be anticipated to have lower wind speeds, more resolved meteorological data would be expected to further enhance the intra-urban variability in the iF and increase the average iF. Furthermore, different patterns of vehicle mix and speed would lead to different amounts of vehicle-induced turbulence, which would influence dispersion on individual road segments. If we were interested in short-term rather than long-term iF, the joint effects of spatially and temporally variable meteorology and spatially variable population patterns would lead to even greater variability. On a related point, incorporating road-specific emissions, while it would have no effect on the hourly intake fractions (which are normalized by emissions), could influence the annual average iF should emissions-weighted hourly values be used. Emissions-weighted averages would most directly correspond with annual average impacts. However, as Figure S-6 indicates, diurnal iF variability is relatively low, and this would have a small effect on our conclusions.

On average, just under half of the iF is reached by 200 m from the midpoint of the roads, though this varies from 0 to 93%. Thus, depending upon the distribution of the population around the road segment, a 200 m modeling domain may or may not be sufficient to capture all impacts (although our regression models indicate that population estimates within 200 m could provide a first approximation of the iF, provided that a constant term is maintained to reflect longer-range populations). To ensure that longer-range impacts could be captured and to facilitate comparability with past modeling efforts, we used a modeling domain of 5000 m. While this is greater than the 1000 m commonly recommended for CALINE (*20*), our findings demonstrate the importance of capturing this domain, at least for some population distributions.

Our previous study using the Source−Receptor matrix at county-level resolution found the mobile source iF captured within counties comprising the Boston Metro Core area to vary between 1.9 and 4.5 per million (*7*). The current study found much greater variability and a higher central value, indicating a potential low bias in the previous study; however, comparisons between different models with different resolution are difficult given the inherent uncertainties in each model. The previous study also found an appreciable contribution of populations outside of the county to total iF (from 29% to 59%). It is possible that the fraction of total exposure captured within 200 m in the present study is overestimated, if populations outside of 5000 m make appreciable contributions to the iF. To the extent that a significant fraction of iF occurs beyond 5000 m, our analysis has overstated variability and underestimated the average iF. However, our mean estimates are of similar magnitude

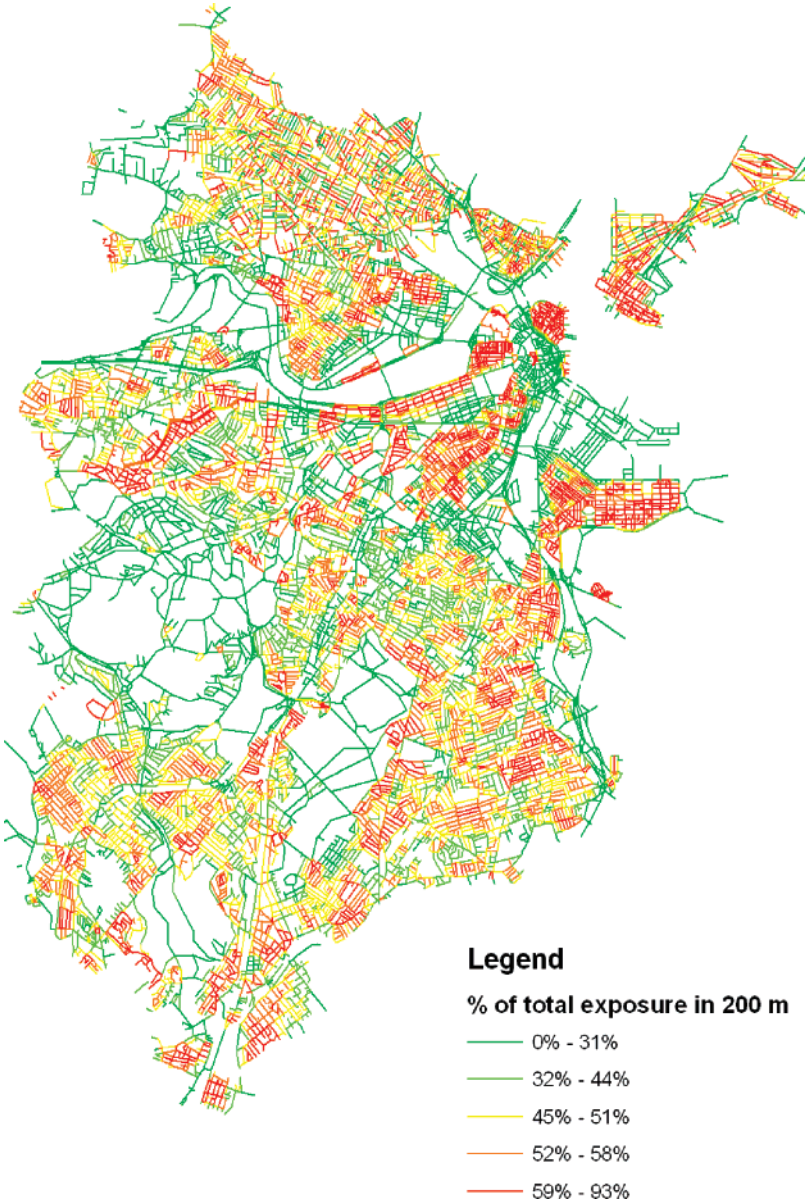

FIGURE 3. Annual average fraction of total exposure reached in 200 m from the road segment.

TABLE 3. Anticipated Effect of Simplifying Assumptions on the Degree of Intra-Urban Variability in Mobile Source Intake Fractions and the Bias in the Average Intake Fraction

	likely direction/importance of influence on annual average iF	
assumption	**iF magnitude**	**iF variability**
exposure to residential populations only (no microenvironments or time-activity patterns)	underestimate/large	underestimate/large
identical meteorology assumed for all road segments, with exclusion of vehicle-induced turbulence	underestimate/medium	underestimate/medium
exclusion of iF beyond 5000 m of the roadway	underestimate/medium	overestimate/small
CAL3QHCR applied in spite of lack of street canyons, performance at low wind speeds	underestimate/small	underestimate/small
no variability in population density at smaller than block group resolution, uniform population density within each annulus	unclear/small	unclear/small
annual iF does not include diurnal variability in emissions	unclear/small	unclear/small
no variability in street configurations	unclear/small	underestimate/medium

as previous estimates with greater spatial scale (*10*, *11*), indicating long-range impacts would not likely be so large as to make intra-urban variability trivial.

Using a line-source model to estimate exposure has the advantage of incorporating both spatial and temporal variability in air pollution levels without dense monitoring networks, which are costly and laborious. However, some unrealistic assumptions must be made regarding Gaussian dispersion patterns (*21*). There are other limitations in the current analysis that must be acknowledged. CAL3QHCR is a simplified dispersion model, so there are obvious uncertainties in the outputs of our analysis. For example,

CAL3QHCR does not handle low wind speed situations. As a result, we had to exclude 21 h of meteorological data where wind speeds were less than 1 m s^{-1}, a minor issue within our analysis but a potentially important one for settings with frequent still winds. The model also tends to overpredict concentrations for parallel-to-the-road wind directions (*13*). We did not exclude these conditions from our analysis, since wind directions within 15° of the road centerline could occur up to one-sixth of the time. In the future, if all road segments are modeled individually, the Horst−Venkatram approximation can be applied that improves the performance of the line-source model for parallel-to-the-road wind directions (*22*).

In our analysis, we used the same street configuration for each road segment, which is clearly not realistic. Road segments in the Boston Metro Core area might exist in tunnels or elevated freeways rather than at grade, and street canyons might also exist. None of these special road types were included in our analysis, partly because of limitations in data inputs and partly because the street-canyon module in CALINE4 was unsuitable for our purposes. Other models might be better equipped to investigate the relationship between exact road configuration and iF (*23*). However, the majority of the road segments fit the typical configuration used. Moreover, the purpose of the analysis was to determine whether intra-urban variability in mobile source primary $PM_{2.5}$ iF existed or not. More detailed modeling of the actual road segment configuration is only expected to increase this heterogeneity. Similarly, CAL3QHCR required the roughness length and settling velocity to be constant over the modeling domain. Varying these parameters by using different modeling domains for each road segment would be expected to increase intra-urban variability in the iF.

Given these limitations, it could be argued that an alternative model should have been employed. CAL3QHCR is one of several deterministic line-source models that exist to evaluate the concentration impacts of motor vehicles. Other deterministic models include APRAC, HIWAY, and TEXIN (*24*). Since CAL3QHCR has been used in the past, is an EPA-recommended model, and allowed for the examination of the sensitivity of outputs to key input parameters, it served our purposes best. Other more computationally intensive numerical, stochastic, computational fluid dynamic (CFD), and artificial neural network methods exist. However, these models could not be feasibly applied to numerous road segments, so CAL3QHCR was most appropriate to the investigation of intra-urban iF variability in the present analysis. Some minor refinements, associated with improvements in CALINE4 relative to CALINE3, might improve our exposure assessment, although this would require additional model development as CALINE4 cannot easily incorporate meteorology across the year.

Obtaining block-level-resolved population estimates around each of the 23 398 road segments was essential in determining whether intra-urban variability in mobile source primary $PM_{2.5}$ iFs exists. However, this only represents residential populations, and people spend much of their time at locations other than their residence. At fine geographic resolution, it may be inadequate to assume that population exposures occur at residential locations. Accounting for workers and transient populations might yield a different iF map than the one depicted in Figure 2, but data were unavailable to formally incorporate time−activity patterns. We would anticipate that estimating exposure-based iF would significantly increase the average value, and would likely increase variability in this setting as well, as many of the areas of high residential population density also have significant business, pedestrian, and commuter activities. Of the above-mentioned assumptions, the focus on residential populations likely contributes the greatest amount of bias (Table 3), although it is aligned with current epidemiological evidence for $PM_{2.5}$.

In conclusion, by using residential population information within 5 km of each road segment in the Boston Metro Core area, the annual average mobile source primary $PM_{2.5}$ intake fraction was found to vary from 0.81 to 53 per million, given an assumption of spatially uniform meteorology and road characteristics. Incorporating more spatially and temporally resolved time−activity and meteorological data would further refine these iF estimates and would be anticipated to increase iF heterogeneity. The contribution of populations close to the road segment to iF varied substantially (between 0 and 93% of the total exposure occurred within 200 m of each road segment), with a non-negligible fraction of the total exposure occurring outside of 1000 m from the road segments. Future dispersion modeling efforts should incorporate both high-resolution near-source modeling and longer-range fate and transport to better determine the magnitude and degree of intra-urban variability in exposure for benefits assessments.

Acknowledgments

This work was supported by EPA/Harvard Center on Ambient Particle Health Effects (R827353) and by the Harvard-NIEHS Center (ES00002). The authors thank Steve Melly for conducting GIS analyses, without which this work would not have been possible; Ying Zhou and Jack Spengler for helpful comments in the framing of the manuscript; and Trinity Consultants for allowing us to use the CAL3QHCR model in the BREEZE software under the student agreement.

Supporting Information Available

Four tables (containing detailed information about meteorological conditions, population information, alternative regression formulations, and other sensitivity analysis), and six figures (depicting a map of the study area and the relationship between hourly intake fractions and fraction of total exposure captured within several radii, wind speed, mixing height, stability class, and hour-of-day). This material is available free of charge via the Internet at http://pubs.acs.org.

Literature Cited

(1) U.S. Environmental Protection Agency. I*nterim Regulatory Impact Analysis for the PM2.5 National Ambient Air Quality Standards*; Office of Air Quality, Planning and Standards: Washington, DC, 2006.
(2) Hitchins, J.; Morawska, L.; Wolff, R.; Gilbert, D. *Atmos. Environ.* **2000**, *34*, 51−59.
(3) Zhu, Y. F.; Hinds, W. C.; Kim, S.; Sioutas, C. *J. Air Waste Manage. Assoc.* **2002**, *52*, 1032−1042.
(4) Janssen, N. A. H.; van Vliet, P. H. N.; Aarts, F.; Harssema, H.; Brunekreef, B. *Atmos. Environ.* **2001**, *35*, 3875−3884.
(5) U.S. Environmental Protection Agency. *Regulatory Impact Analysis - Control of Air Pollution from New Motor Vehicles: Tier 2 Motor Vehicle Emissions Standards and Gasoline Sulfur Control Requirements*; Office of Air and Radiation: Washington, DC, 1999.
(6) Bennett, D. H.; McKone, T. E.; Evans, J. S.; Nazaroff, W. W.; Margni, M. D.; Jolliet, O.; Smith, K. R. *Environ. Sci. Technol.* **2002**, *36*, 206A−211A.
(7) Greco, S. L.; Wilson, A. M.; Levy, J. I. *Atmos. Environ.* **2007**, *41*, 1011−1025.
(8) Marshall, J. D.; Teoh, S. K.; Nazaroff, W. W. *Atmos. Environ.* **2005**, *39*, 1363−1371.
(9) Marshall, J. D.; Riley, W. J.; McKone, T. E.; Nazaroff, W. W. *Atmos. Environ.* **2003**, *37*, 3455−3468.
(10) Evans, J. S.; Wolff, S. K.; Phonboon, K.; Levy, J. I.; Smith, K. R. *Chemosphere* **2002**, *49*, 1075−1091.
(11) Nigge, K.-M. *Int. J. Life Cycle Assess.* **2001**, *6*, 257−264.
(12) U.S. Environmental Protection Agency. *User's Guide to CAL3QHC Version 2.0: A Modeling Methodology for Predicting Pollutant Concentrations Near Roadway Intersections*; Office of Air Quality Planning and Standards: Washington, DC, 1995.

(13) Benson, P. E. *Atmos. Environ.* **1992**, *26*, 379−390.
(14) Sivacoumar, R.; Thanasekaran, K. *J. Environ. Eng.-Asce* **2001**, *127*, 524−530.
(15) Levitin, J.; Harkonen, J.; Kukkonen, J.; Nikmo, J. *Atmos. Environ.* **2005**, *39*, 4439−4452.
(16) California Department of Transportation. *CALINE3 - A Versatile Dispersion Model for Predicting Air Pollutant Levels Near Highways and Arterial Streets*; Office of Transportation Laboratory: Sacramento, CA, 1979.
(17) U.S. Environmental Protection Agency. *Addendum to the User's Guide to CAL3QHC Version 2.0 (CAL3QHCR User's Guide)*; Office of Air Quality Planning and Standards: Washington, DC, 1995.
(18) Seinfeld, J. H.; Pandis, S. N. *Atmospheric Chemistry and Physics*; John Wiley & Sons, Inc.: New York, 1998.
(19) Hanna, S.; White, J.; Zhou, Y.; Kosheleva, A. In *6th Urban Environment Conference of the American Meteorological Society*; Atlanta, GA, 2006.
(20) Caltrans. *CALINE4 − A Dispersion Model for Predicting Air Pollutant Concentrations Near Roadways*; Caltrans Division of New Technology and Research: Sacramento, CA, 1989.
(21) Jerrett, M.; Arain, A.; Kanaroglou, P.; Beckerman, B.; Potoglou, D.; Sahsuvaroglu, T.; Morrison, J.; Giovis, C. *J. Exposure Anal. Environ. Epidemiol.* **2005**, *15*, 185−204.
(22) Venkatram, A.; Horst, T. W. *Atmos. Environ.* **2006**, *40*, 2401−2408.
(23) Vardoulakis, S.; Fisher, B. E. A.; Pericleous, K.; Gonzalez-Flesca, N. *Atmos. Environ.* **2003**, *37*, 155−182.
(24) Nagendra, S. M. S.; Khare, M. *Atmos. Environ.* **2002**, *36*, 2083−2098.

Received for review September 15, 2006. Revised manuscript received May 14, 2007. Accepted June 11, 2007.

ES062213F